Published in final edited form as:

J Math Biol. 2019 July ; 79(2): 571–594. doi:10.1007/s00285-019-01369-w.

Bidirectional sliding of two parallel microtubules generated by multiple identical motors

Jun Allard[1], **Marie Doumic**[2], **Alex Mogilner**[3], **Dietmar Oelz**[4]

[1]Department of Mathematics, University of California Irvine, Irvine, CA, USA

[2]Inria, UPMC Univ Paris 06, Lab. J.L. Lions UMR CNRS 7598, Sorbonne Universités, Paris, France

[3]Courant Institute of Mathematical Sciences, New York University, New York, NY 10012, USA

[4]School of Mathematics and Physics, The University of Queensland, St. Lucia, QLD 4072, Australia

Abstract

It is often assumed in biophysical studies that when multiple identical molecular motors interact with two parallel microtubules, the microtubules will be crosslinked and locked together. The aim of this study is to examine this assumption mathematically. We model the forces and movements generated by motors with a time-continuous Markov process and find that, counter-intuitively, a tug-of-war results from opposing actions of identical motors bound to different microtubules. The model shows that many motors bound to the same microtubule generate a great force applied to a smaller number of motors bound to another microtubule, which increases detachment rate for the motors in minority, stabilizing the directional sliding. However, stochastic effects cause occasional changes of the sliding direction, which has a profound effect on the character of the long-term microtubule motility, making it effectively diffusion-like. Here, we estimate the time between the rare events of switching direction and use them to estimate the effective diffusion coefficient for the microtubule pair. Our main result is that parallel microtubules interacting with multiple identical motors are not locked together, but rather slide bidirectionally. We find explicit formulae for the time between directional switching for various motor numbers.

Keywords

Tug-of-war; Molecular motors; Intra-cellular transport; Reversal rate

Mathematics Subject Classification

46N60; 92C05; 92C37; 60J28; 60J80

✉Dietmar Oelz, d.oelz@uq.edu.au.

1 Introduction

Many fundamentally important examples of intracellular transport are driven by molecular motor proteins that drag cargo (vesicles and organelles) on polar tracks within cells by transducing chemical energy into mechanical forces and movements (Rogers and Gelfand 2000). More often than not, the cargo is driven by multiple, not single, motors (Gross et al. 2007). If all the motors bound to the cargo are of the same kind, then the motors normally synergize and hold on to the cargo for a longer time, driving it farther and faster (Gross et al. 2007; McKinley et al. 2012). In some cases, however, two opposing kinds of motors are bound to the cargo. The most frequent example is when a vesicle or a pigment particle has multiple kinesin and dynein motors on its surface, which interact with a long microtubule (MT) fiber (Nascimento et al. 2003). A single kinesin motor tends to move toward the MT plus end, while a single dynein motor moves to the MT minus end. Each of these opposite-polarity motors is characterized by two important mathematical relations: a force-velocity and a force-detachment relation. Namely, if unopposed, a motor moves to respective microtubule end with a certain 'free' speed, but if a load force opposes this movement, the speed decreases as a certain measured function of the force (Svoboda and Block 1994). The motor also dissociates from the MT with a rate which is a function of the force, often an increasing function (Kunwar et al. 2011).

When a few kinesins and a few dyneins are bound to the cargo, a pioneering model (Klumpp and Lipowsky 2005; Müller et al. 2008) explained the tug-of-war phenomenon previously observed experimentally (Gross et al. 2002; Kural et al. 2005). Specifically, once in a while, kinesins 'win' when a majority of them associate with the MT and move to the plus end. The collective kinesin action then applies a great force to few dyneins associated with the MT, and this great force leads to rapid detachment of all dyneins. However, as the motors' attachment and detachment are stochastic, many kinesins detach infrequently, allowing a few dyneins to attach, and then kinesins lose the majority and dyneins temporarily win, now applying a great load force to kinesins, until the next great fluctuation restores the kinesin majority. Repeated many times, this process results in a bidirectional movement of the cargo. An elegant mathematical model (Klumpp and Lipowsky 2005; Müller et al. 2008) predicted that the frequency of these reversals depends on the motor numbers. Many subsequent modeling studies, mentioned in the Discussion, refined and developed this model further.

There are also ubiquitous cases in cell biology when the cargo is, effectively, one MT, to which motors bind with their cargo domain and drive it on a second MT (Fig. 1). For example, this is how short MTs are thought to be transported on long MTs in long axons of nerve cells (Craig et al. 2017). Another important situation is when two MTs of similar lengths are sliding relative to one another due to the action of motors crosslinking them; this was observed in mitotic spindles (Wollman et al. 2008) and in nascent dendrites, axons and so-called cellular processes (del Castillo et al. 2015; Oelz et al. 2018). This situation would be straightforward if a single motor was driving one MT on another. However, much more likely, multiple motors *of the same kind* crosslink the MTs (Fig. 1).

Let us consider possible MT-motor configurations. First, let two MTs be anti-parallel (Fig. 1a). Then, whether two identical motors are bound with their cargo domains on the same MT or not, the motors' actions are coherent, leading to the anti-parallel sliding of the MT pair. This phenomenon is at the core of key cell biological processes such as spindle and axon elongation (Sharp et al. 2000; Lu et al. 2013). Second, let two MTs be parallel (Fig. 1b). In that case, if all *identical* motors are bound with their cargo domains on the same MT, then the MT pair slides. However, as the motor attachments are random, it is more likely that only a fraction of motors attach with their cargo domains to the first MT and pull the second MT to the left (Fig. 1b). Meanwhile, the rest of the motors attach with their cargo domains to the second MT and pull the first MT also to the left (Fig. 1b) (or, if MT1 is considered as the base, MT2 is pulled to the left/right by these two fractions of the motors). If two opposing motor fractions consist of equal motor numbers, all motors will be stalled, and the MT pair will be effectively locked together. This is exactly what many experimental studies assumed either explicitly (Lu and Gelfand 2017) or implicitly (Wollman et al. 2008).

It is easy to imagine though that stochastic effects will break symmetry between the opposing kinesins, and then some motors with cargo domains bound to the same MT will be in majority. Then, these motors apply a great force to a small number of motors with cargo domains on another MT, the motors in minority detach, and the tug-of-war cycle ensues. Intuitively, the parallel MT pair then will not be locked together, but rather slide bidirectionally. In this study, we aim to quantify the resulting tug-of-war, namely, to calculate how often the MT sliding will change direction and what will be the resulting run-length and effective diffusion coefficient.

Our main result is that the expected time between MTs' switching directions can be estimated as the expected hitting time for a reversible birth and death process. We find several asymptotic formulae for a large total number of motors and strong load dependence of the detachment rates, which allow us to estimate the effective diffusion coefficient.

In the first section, we present the mathematical model and investigate its asymptotic behavior analytically. In the second section, we introduce the expected hitting times for the underlying Markov process, and discuss their relation to the switching times in the third section. We then investigate approximate model solutions for a large total number of motors in section four, and further approximations using Laplace's method in the fifth and last section.

2 Mathematical model

We consider identical molecular motors acting in one of two opposite directions. N is the number of molecular motors pushing in positive direction, M is the number of motors pushing in negative direction. The maximal number of motors is given by $K \geq N + M$. Specifically, the model assumes that each motor bound to a MT occupies a segment of a certain length. Thus, M and N are the total numbers of motors crosslinking two parallel MTs of unit length. K is the maximal motor number that fits the overlap.

We model the molecular motors by force-velocity relations in which the force exerted by a single motor pushing in positive, respectively negative direction is given by

$$f^+ = F_s\left(1 - \frac{\Delta v}{V_m}\right), \quad f^- = F_s\left(-1 - \frac{\Delta v}{V_m}\right),$$

where Δv is the velocity of the cargo (the relative velocity of parallel MTs, respectively) and F_s and V_m are stall force and free moving velocity of a single motor. Note that f^+represents the force exerted by a motor sliding in positive direction, whereas $f^- = -F_s\left(1 - \frac{-\Delta v}{V_m}\right)$ corresponds to the force exerted by a motor acting in negative direction. Here $-\Delta v$ plays the role of the sliding velocity in negative direction.

We choose the simplest possible model to determine Δv, namely instantaneous force balance of all the motors involved: $Nf^+ + Mf^- = 0$, i.e.

$$F_s N\left(1 - \frac{\Delta v}{V_m}\right) + F_s M\left(-1 - \frac{\Delta v}{V_m}\right) = 0\,.$$

This implies:

$$\frac{\Delta v}{V_m} = \frac{N - M}{N + M},$$

(2.1)

and therefore

$$f^+(M,N) = F_s\frac{2M}{N+M}, \quad f^-(M,N) = F_s\frac{2N}{N+M},$$

implying $f^+\left(M,N\right) = f^-\left(N,M\right)$.

Provided that free binding sites on the MTs' overlap are available, i.e. $N + M < K$, we assume that molecular motors attach to the two MTs at the given rate β. They are equally likely to attach with their motor domain to one or to the other MT. The motors also detach from the pairs of MTs at certain rates, namely those sliding in positive direction detach with rate $\xi^+$and those sliding in negative direction with rate ξ^-. We assume that off-rates increase whenever motor proteins experience mechanical resistance according to Bell's law (Bell 1978),

$$\begin{aligned}\xi^+\left(M,N\right) &= N\bar{\kappa}_0\exp\left(\frac{f^+(M,N)}{f_0}\right) = N\bar{\kappa}_0\exp\left(\gamma\frac{M}{N+M}\right)\\ \xi^-\left(M,N\right) &= M\bar{\kappa}_0\exp\left(\frac{f^-(M,N)}{f_0}\right) = M\bar{\kappa}_0\exp\left(\gamma\frac{N}{N+M}\right)\end{aligned}$$

(2.2)

where f_0 is the detachment force of kinesin and $\bar{\kappa}_0$ is its forceless detachment rate. We use the short notation $\gamma = 2F_s/f_0$ (see Table 1). For symmetry reasons it again holds that $\xi^-(M,N) = \xi^+(N,M)$.

Note that we neglect the environmental drag on the MTs sliding in a direction parallel to their axis. Indeed, the environmental drag acting on a microtubule of 5 μm length sliding at the free moving velocity of kinesin (see Table 1) can be estimated (Oelz et al. 2018) as ~ 2pN. This drag is smaller than the stall force of even a single kinesin motor and can therefore be neglected in a system where a few motors act simultaneously.

To reduce the size of the phase space (Fig. 2) we assume that the attachment rate β is large and therefore reattachment of a new motor is immediate. As a consequence the total number of motors always takes its maximal value: $N + M = K$. This reduces the original triangular phasespace (Fig. 2a) to a linear chain of possible states (Fig. 2b). As a consequence, the turnover of motors is governed by motor detachment: as fast as one motor detaches, another one, of an arbitrary polarity, takes its place (see Fig. 3).

In this simplified scenario we write $i = N$ for the number of motors pulling in the positive direction, while the number of motors pulling in the negative direction is given by $K - i$. The corresponding time-continuous Markov Process with state variable $i \in \{0,1,\ldots,K\}$ corresponds to a classical birth–death reversible process (Anderson 1991). We denote by $\kappa_i^+ = \frac{1}{2}\xi^-(K-i,i)$ for $0 \le i < K$ the rate at which one of the $K - i$ motors pulling in the negative direction switches to the positive direction, i.e. the state transitions from i to $i + 1$. Note that the factor $\frac{1}{2}$ reflects the 50% chance that a detached motor is replaced by a motor in the opposite direction. Likewise, $\kappa_i^- = \frac{1}{2}\xi^+(K-i,i)$ is the rate at which one of the i motors pulling in the positive direction is replaced by a motor in the negative direction, i.e. the state transitions from i to $i - 1$. The rates are given by the detachment rates of the general model (2.2) which, using the new notation, read:

$$\kappa_i^- = i\,\kappa_0 \exp\left(\gamma\left(\frac{K-i}{K}\right)\right), \quad \kappa_i^+ = (K-i)\,\kappa_0 \exp\left(\gamma\frac{i}{K}\right), \tag{2.3}$$

where $\kappa_0 = 1/2\bar{\kappa}_0$. Note that these rates are proportional to the number of motors which are potentially replaced while the force depends on the number of motors pulling in the opposite direction. Again, by symmetry it holds that $\kappa_i^- = \kappa_{K-i}^+$ for $1 \le i \le K$.

The infinitesimal generator of the process is given by $\mathbf{Q} = (q_{ij})_{1 \le i,j \le K}$ with

$$q_{ij} = \kappa_i^+ \delta_{j=i+1} + \kappa_i^- \delta_{j=i-1} - (\kappa_i^+ + \kappa_i^-)\delta_{i=j}, \quad 0 \le i,j \le K,$$

with the convention $\kappa_K^+ = \kappa_0^- = 0$. This is a tridiagonal matrix given by (here for $K = 4$)

$$\mathbf{Q} = \begin{pmatrix} -\kappa_0^+ & \kappa_0^+ & 0 & 0 & 0 \\ \kappa_1^- & -(\kappa_1^- + \kappa_1^+) & \kappa_1^+ & 0 & 0 \\ 0 & \kappa_2^- & -(\kappa_2^- + \kappa_2^+) & \kappa_2^+ & 0 \\ 0 & 0 & \kappa_3^- & -(\kappa_3^- + \kappa_3^+) & \kappa_3^+ \\ 0 & 0 & 0 & \kappa_4^- & -\kappa_4^- \end{pmatrix}. \tag{2.4}$$

We denote by $\mathbf{p}(t) = (p_i(t))_{0 \le i \le K}$ with $\sum_{i=0}^{K} p_i(t) = 1$ the time-dependent probabilities that the system is in state i, i.e. that there are i motors pulling in the positive direction and therefore $K - i$ motors pulling in negative direction. As a consequence, they satisfy the system of forward Chapman–Kolmogorov equations $d\mathbf{p}/dt = \mathbf{Q}^t\mathbf{p}(t)$. In detail,

$$\frac{dp_i}{dt} = -(\kappa_i^+ + \kappa_i^-)p_i + \kappa_{i-1}^+ p_{i-1} + \kappa_{i+1}^- p_{i+1}, \quad p_i(0) = p_i^0, \quad 0 \le i \le K, \tag{2.5}$$

with the convention, as previously for the transition rates, $p_{-1} = p_{K+1} = 0$. We have the following classical result (Grimmett et al. 2001):

Proposition 1 *Let $K \ge 2, \kappa_{i-1}^+ > 0$ and $\kappa_i^- > 0$ for $1 \le i \le K$, with the convention $\kappa_0^- = \kappa_K^+ = 0$. Let $p_i^0 \ge 0$, with $\sum_{i=0}^{K} p_i^0 = 1$. The unique solution $\mathbf{p}(t)$ to the system (2.5) converges exponentially fast towards the invariant measure $\overline{\mathbf{p}} := (\overline{p}_i)_{0 \le i \le K}$ defined by*

$$\overline{p}_i := \frac{\pi_i}{\sum_{k=0}^{K} \pi_i}, \quad \text{where} \quad \pi_0 := 1, \quad \pi_i := \prod_{k=1}^{i} \frac{\kappa_{k-1}^+}{\kappa_k^-}. \tag{2.6}$$

For the specific form of κ_i^+, κ_i^- given by (2.3) it holds that

$$\pi_i = \prod_{k=1}^{i} \frac{\exp\left(\gamma \frac{k-1}{K}\right)}{\exp\left(\gamma \frac{K-k}{K}\right)} \frac{K-k+1}{k} = \frac{K!}{i!(K-i)!} \exp\left(K\gamma \frac{i}{K}\left(\frac{i}{K} - 1\right)\right).$$

Proof Proposition 1 is an immediate consequence of the Perron–Frobenius theorem (Saloff-Coste 1997). To find the unique positive steady state distribution $\overline{\mathbf{p}} = (\overline{p}_i)_{0 \le i \le K}$, we write $\mathbf{Q}^t\overline{\mathbf{p}} = 0$ as a recursion relation for a given $\overline{p}_0$:

$$\overline{p}_1 = \frac{\kappa_0^+}{\kappa_1^-}\overline{p}_0, \quad \overline{p}_i = \frac{(\kappa_{i-1}^+ + \kappa_{i-1}^-)\overline{p}_{i-1} - \kappa_{i-2}^+ \overline{p}_{i-2}}{\kappa_i^-} = \frac{\kappa_{i-1}^+}{\kappa_i^-}\overline{p}_{i-1} \quad \text{for} \quad 1 < i < K, \text{ and} \quad \overline{p}_K = \frac{\kappa_{K-1}^+}{\kappa_K^-}\overline{p}_{K-1}.$$

This implies that $\overline{p}_i = \left(\prod_{k=1}^{i} \frac{\kappa_{k-1}^{+}}{\kappa_k^{-}}\right)\overline{p}_0$ for $i \geq 1$, and using relation $\sum_{i=0}^{K} \overline{p}_i = 1$ to determine $\overline{p}_0$, we obtain the invariant measure defined by (2.6). For κ_i^{+}, κ_i^{-} defined by (2.3), we simply compute:

$$\prod_{k=1}^{i} \frac{\exp\left(\gamma \frac{k-1}{K}\right)}{\exp\left(\gamma \frac{K-k}{K}\right)} = \exp\left(\gamma \sum_{k=1}^{i} \left(\frac{k-1}{K} - \frac{K-k}{K}\right)\right) = \exp\left(K\gamma \frac{i}{K}\left(\frac{i}{K} - 1\right)\right).$$

□

This typically corresponds to a bimodal distribution, symmetric with respect to $\frac{K}{2}$, as shown in Fig. 4b for our standard set of parameters in Table 1.

Let us go back now to our original question of how frequently the MTs change direction, which is linked to the effective rate of diffusion of the random walk of one MT relative to the other (Fig. 5a).

The tug-of-war stabilizes the dominance of one of the two opposing groups of motors. Switching between dominance of one group to dominance of the other group, which corresponds to switching direction, is a rare event as illustrated by the simulation shown in Fig. 4a. In this simulation, the mean time for directional switching is $\tau = 162\,\mathrm{s}$. In a tug-of-war situation, most of the time one group of motors will dominate and the relative velocity will be given by almost the free moving velocity V_m, either in positive or negative direction. The resulting estimate for the diffusion coefficient will be given by $\frac{1}{2} \times$ run-length $\times$ velocity, i.e. $\frac{1}{2} V_m^2 \tau = 26.3\,\mu\mathrm{m}^2/\mathrm{s}$. In the stochastic simulation (Fig. 5b), however, we find a diffusion coefficient of $17.4\,\mu\mathrm{m}^2/\mathrm{s}$. Most of the discrepancy is caused by the fact that the mean relative velocity is indeed slower than V_m. A better estimate for the mean relative velocity uses the fact that the stationary distribution in Fig. 4b has maxima at $J_{\max} = 33$ and $K - J_{\max} = 2$. The relative velocity at these states, according to (2.1), will be $\Delta v = V_m \times 31/35 = 0.5\,\mu\mathrm{m/s}$, and the corresponding estimate for the diffusion coefficient $\frac{1}{2} \times 0.5^2 \times \tau = 20.6\,\mu\mathrm{m}^2/\mathrm{s}$ agrees well with the numerical result. Further estimates for various values of γ are listed in Table 2.

Note that directional switches for $\gamma = 4$ are very rare, and we therefore compute the expected time for switching directly from (3.3) for $J_{\max} = K$, since the stationary distribution has its maxima at 0 and K.

Note also that while we overestimate the diffusion rate for the larger values of γ, we underestimate the rate for the borderline case $\gamma = 2$, due to the fact that the stationary distribution is wide-spread.

Finally, in the case without actual tug-of-war where $\gamma = 0$ and where the stationary distribution has a single peak at $K/2$ (K even) or $(K \pm 1)/2$ (K odd), respectively, we only

get a very rough estimate of the diffusion coefficient depending on which state we take as equivalent of $J_{\max}$. Picking either $J_{\max} = 14$ or $J_{\max} = 16$, we get the interval of diffusion rates shown in Table 2. Note that Fig. 8a below provides a comparison of stationary distributions (continuous approximation) for different values of γ.

Because of these considerations, our strategy to quantify the switching time between directions is as follows: First, we focus on the expected first hitting time τ_{IJ} which is the expected time for the process to proceed from state I to state J. In a typical situation, where state I characterizes a majority of motors pulling in one direction, while state J refers to a state in which most motors pull in the opposite direction (e.g. take $J = J_{\max}$ and $I = K - J_{\max}$), the expected hitting time will be a good estimate for the time necessary to switch directions.

3 Expected hitting times

To compute the expected time after which the cargo switches directions, we analyze *the first hitting time* in the context of this random process.

A linear system of equations, which describes the expected time τ_{IJ} to go from state I to state J, can be derived as follows [see, e.g. Norris (1997)]: we modify the generator $\mathbf{Q}$ assuming that the state J is absorbing. To this end, we delete both the column and the row of the generator, which correspond to state J, in order to obtain the generator $\mathbf{Q}_J$. For $K = 4$, the generator matrix $\mathbf{Q}_3$ has the form:

$$Q_3 = \begin{pmatrix} -\kappa_0^+ & \kappa_0^+ & 0 & 0 \\ \kappa_1^- & -(\kappa_1^- + \kappa_1^+) & \kappa_1^+ & 0 \\ 0 & \kappa_2^- & -(\kappa_2^- + \kappa_2^+) & 0 \\ 0 & 0 & 0 & -\kappa_4^- \end{pmatrix}.$$

Note that the state space of this $(K-1)$-dimensional process are the states $\{1, \ldots, J-1, J+1, \ldots, K\}$. The solution of this process can be written as $\mathbf{P}_J(t) = \exp(t\mathbf{Q}_J)$ where $P_J(t)$ is the transition matrix function for the process absorbed in state J (its row I corresponds to a process which has started in the state I (out of $K-1$ states in total), namely to the probabilities of finding this process in each one of the non-absorbing states).

Therefore, $\mathbf{P}_J(t)(1,1\ldots,1)^T = \exp(t\mathbf{Q}_J)(1,1\ldots,1)^T = (\mathbb{P}_i[T_{IJ} > t])_I$ is the vector of survival probabilities, i.e T_{IJ} is the first hitting time of a process which started in state I targeting state J. This approach leads us to the following result, which is also classical (Grimmett et al. 2001).

Proposition 2 *Let $K \geq 2$ be an integer, and $\kappa_i^+ > 0, \kappa_{i+1}^- > 0$ are positive real parameters for $0 \leq i \leq K-1$, with the convention $\kappa_0^- = \kappa_K^+ = 0$. Let $\mathbf{Q}$ be the infinitesimal generator of a stochastic process defined by* (2.4). *Denoting by τ_{IJ} the expected hitting time to go from the state I to the state $J \neq I$, the hitting times are the unique solution to the following linear system:*

$$\tau_{IJ} = \frac{1}{\kappa_I^+ + \kappa_I^-} + \frac{\kappa_I^+}{\kappa_I^+ + \kappa_I^-}\tau_{I+1,J} + \frac{\kappa_I^-}{\kappa_I^+ + \kappa_I^-}\tau_{I-1,J}, \quad 0 \le I \le K, \quad I \ne J\,. \tag{3.1}$$

By recursion, we obtain

$$\tau_{IJ} = \sum_{j=I}^{J-1}\sum_{i=0}^{j}\frac{1}{\kappa_i^+}\prod_{k=i+1}^{j}\frac{\kappa_k^-}{\kappa_k^+} = \sum_{j=I}^{J-1}\frac{1}{\kappa_j^+\frac{\overline{p}_j}{\sum_{i=0}^{j}\overline{p}_i}}\,. \tag{3.2}$$

In particular, τ_{0J} *is given by*

$$\tau_{0J} = \sum_{j=0}^{J-1}\sum_{i=0}^{j}\frac{1}{\kappa_i^+}\prod_{k=i+1}^{j}\frac{\kappa_k^-}{\kappa_k^+} = \sum_{j=0}^{J-1}\frac{1}{\kappa_j^+\frac{\overline{p}_j}{\sum_{i=0}^{j}\overline{p}_i}}\,. \tag{3.3}$$

Remark 1 In formulae (3.3) and (3.2), we notice that the denominator is a weighted transition rate to go from j to $j+1$, i.e. rate weighted with the conditional probability (in equilibrium) to be in state j, under the condition to be in one of the states $\le j$.

Proof This result is well-known; we recall here briefly the proof for the sake of completeness. The distribution of hitting times for the absorbing state J is given by $\mathbf{f}_J(t) = -d/dt\exp(t\mathbf{Q}_J)(1,1\ldots,1)^T$ where $\mathbf{f}_J = (f_{IJ})_{I\ne J}$. We compute the expected hitting times $\boldsymbol{\tau}_J = (\tau_{1,J},\ldots,\tau_{J-1,J},\tau_{J+1,J},\ldots\tau_{K,J})^T$ as

$$\begin{aligned}\boldsymbol{\tau}_J &= (\mathbb{E}[T_{IJ}])_{I\ne J} = \int_0^\infty t\mathbf{f}_J dt = \int_0^\infty \exp(tQ_J)dt\big(1,1\ldots,1\big)^T\\ &= -Q_J^{-1}\big(1,1\ldots,1\big)^T.\end{aligned}$$

Therefore, the expected hitting times satisfy the equation $\mathbf{Q}_J\boldsymbol{\tau}_J = -(1,1\ldots,1)^T$. This implies equation (3.1), which states that the expected time to go from state I to state J is the expected time to leave state I plus the times to reach the final state from either the possible next states $I-1$ or $I+1$ weighted by the respective probabilities to enter those states. Let us first focus on the case $I < J$. We find that

$$\begin{aligned}&\tau_{0J} = \tau_{1J} + \frac{1}{\kappa_0^+}, \tau_{1J} = \frac{1}{\kappa_1^+ + \kappa_1^-}(1 + \kappa_1^+\tau_{2J} + \kappa_1^-\tau_{0J})\\ &= \frac{1}{\kappa_1^+ + \kappa_1^-}\left(1 + \kappa_1^+\tau_{2J} + \kappa_1^-\left(\tau_{1J} + \frac{1}{\kappa_0^+}\right)\right)\\ &\Longrightarrow \tau_{1J} = \tau_{2J} + \frac{1}{\kappa_1^+} + \frac{1}{\kappa_0^+}\frac{\kappa_1^-}{\kappa_1^+},\\ &\text{etc}\,.\end{aligned}$$

and, bootstraping these identities, we obtain a recursive formula expressing τ_{IJ} in terms of $\tau_{I+1,J}$,

$$\tau_{IJ} = \tau_{I+1,J} + \sum_{i=0}^{I} \frac{\prod_{k=i+1}^{I} \kappa_k^-}{\prod_{k=i}^{I} \kappa_k^+} = \tau_{I+1,J} + \sum_{i=0}^{I} \frac{1}{\kappa_i^+} \prod_{k=i+1}^{I} \frac{\kappa_k^-}{\kappa_k^+}, \quad 0 \le I \le J-2,$$

where we define $\prod_{\varnothing} = 1$, where $\varnothing$ denotes the empty set. Since $\tau_{JJ} = 0$, we have

$$\tau_{J-1,J} = \frac{1}{\kappa_{J-1}^+ + \kappa_{J-1}^-} + \frac{\kappa_{J-1}^-}{\kappa_{J-1}^+ + \kappa_{J-1}^-} \tau_{J-2,J},$$

and by the recursion formula we find

$$\tau_{J-2,J} = \tau_{J-1,J} + \sum_{i=0}^{J-2} \frac{1}{\kappa_i^+} \prod_{k=i+1}^{J-2} \frac{\kappa_k^-}{\kappa_k^+},$$

so that

$$\tau_{J-1,J} = \frac{1}{\kappa_{j-1}^+ + \kappa_{j-1}^-} + \frac{\kappa_{j-1}^-}{\kappa_{j-1}^+ + \kappa_{j-1}^-} \left(\tau_{j-1,J} + \sum_{i=0}^{J-2} \frac{1}{\kappa_i^+} \prod_{k=i+1}^{J-2} \frac{\kappa_k^-}{\kappa_k^+} \right),$$

and finally we obtain

$$\tau_{J-1,J} = \frac{1}{\kappa_{J-1}^+} \left(1 + \kappa_{J-1}^- \sum_{i=0}^{J-2} \frac{1}{\kappa_i^+} \prod_{k=i+1}^{J-2} \frac{\kappa_k^-}{\kappa_k^+} \right) = \sum_{i=0}^{J-1} \frac{1}{\kappa_i^+} \prod_{k=i+1}^{J-1} \frac{\kappa_k^-}{\kappa_k^+}.$$

By an immediate recursion, we deduce that

$$\tau_{IJ} = \sum_{j=I}^{J-1} \sum_{i=0}^{j} \frac{1}{\kappa_i^+} \prod_{k=i+1}^{j} \frac{\kappa_k^-}{\kappa_k^+}, \quad 0 \le I \le J-1.$$

The last formula comes directly by interpreting the products and using the definition of $\overline{p}_i$ and $\overline{p}_j$.

For $I > J$, we can do exactly the same computations, replacing indices k by indices $K - k$ and rates $\kappa_k^+$by rates κ_k^-(we can also do this simply by considering a process inverting the numbering of the states and applying the previous formula to this equivalent process). We obtain:

$$\tau_{IJ} = \sum_{n=J+1}^{I} \sum_{k=n}^{K} \frac{1}{\kappa_k^-} \prod_{l=n}^{k-1} \frac{\kappa_l^-}{\kappa_l^+}, \quad J+1 \le I \le K.$$

□

4 Hitting time interpretation of tug-of-war

We are interested in the average time it takes a system to switch direction, i.e. the time it takes the smaller group of antagonistic molecular motors to become dominant. There is no obvious definition for what that means and one could arbitrarily define a specific amount of motors to be the threshold which defines when the transition is accomplished.

To illustrate this point, let us take as a first definition of the switching time the mean time for the majority of motors to change from left to right or vice versa. In our model, where the states in the center of the state space have to be passed through to change direction, we might look at $\tau_{K/2-1,K/2+1} = \tau_{K/2+1,K/2-1}$ in the case of an even number of motors, or $\tau_{(K-1)/2,(K+1)/2}$ in the case of an odd number of motors. By doing so, we count a very high number of very short-range switches, as shown in Fig. 6. This is due to the fact that these mid-points in the state space are unstable for $\gamma > 2$, leading to possibly several changes of direction in a very short time, before leaving this unstable zone and reaching more stable states, where the direction will remain unchanged for a while. In the histogram for the log scale of hitting times shown in Fig. 6 we identify a two-peak distribution, one for very short times—when the system lingers around $\frac{K}{2}$ (opposing motors are balanced), and the other for longer times —when the system lingers in the relatively stable states at the left end of the state space (most of the motors are pulling in the same direction), before transitioning to the right end of the state space. During the very short switching times, the MTs barely move relative to one another. Respective switches in direction are therefore hardly observable.

We will thus accept the definition of the switching time being the expected time to go from the state near one of the two maxima of the stationary distribution to the state near the other maximum. It turns out that the expected hitting times are fairly insensitive to variations of the state of the origin, I, (as long as we stay away from the state at the center of the state space, $K/2$) and to variations of the destination state, J, (as long as we keep enough distance from the transition region around the center of the state space, $K/2$, and from the extreme end of the state space at K).

Note that even if a trajectory starts at an extreme state (either 0 or K), it will move into the region around the nearest maximum of the stationary distribution almost immediately. Computing the expected time to go from any of those states to a state far on the other side of the transition region around $K/2$ will always give approximately the same time, unless the destination is at the extreme other end of the state space. Especially for smaller values of γ, reaching that extreme end is a rare event and therefore computing the expected time to reach the extreme end would overestimate the time necessary to settle in around a state where the antagonistic group of motors is dominant. This is illustrated by Fig. 7a, which shows the steep increase of the transition time at $J = K - 1 = 34$ and $J = K = 35$, while the values of τ_{0J} for $J = 30$ appear to be a good estimate for the switching time.

Another alternative is to consider the expected time to go from the extreme state 0 to the transition states in the center of the state space. This implies that the time to settle in once the transition state $K/2$ (K even) or $(K \pm 1)/2$ is reached can be neglected. In addition, we have to take into account that at this point the process may fall back to a state where the originally dominant group of motors is again dominant or the previously antagonistic group of motors may become dominant. Both scenarios might happen with equal probability, therefore an approximation for the switching time is given by (here for K even)

$$\frac{1}{2}\times\tau_{0\frac{K}{2}}+\frac{1}{4}\times 2\tau_{0\frac{K}{2}}+\frac{1}{8}\times 3\tau_{0\frac{K}{2}}+\ \ldots.\ =2\tau_{0\frac{K}{2}},$$

which states that the system switches direction either immediately after reaching the transition state with probability 1/2, or after falling back and reaching the transition state for the second time (now with probability 1/4), etc.

A numerical comparison of the two approaches for $K = 35$ shows that the predictions indeed coincide for γ large enough. Even for smaller γ, when the time to settle-in is not negligible, the deviations in log-scale are small (Fig. 7b).

5 Continuous approximation

We are now interested in finding a continuous approximation of these formulae when the total number of motors K becomes large. To this end, we use the definitions $\kappa_k^- = k\kappa_0\exp\left(\gamma\left(1-\frac{k}{K}\right)\right)$ and $\kappa_k^+ = \left(K-k\right)\kappa_0\exp\left(\gamma\frac{k}{K}\right)$, and we approximate sums by integrals.

Let us first approximate the steady state.

Proposition 3 *Under the assumptions of Proposition* 2 *and using the definitions of* κ_k^- *and* κ_k^+ *given in* (2.3), *we obtain the following approximation of the steady state as* K *tends to infinity*,

$$\overline{p}_i := \frac{\pi_i}{\sum_{k=0}^{K}\pi_i}, \quad \pi_0 := 1, \quad \pi_i = \exp\left(-Kf\left(\frac{i}{K}\right)-h\left(\frac{i}{K}\right)-\frac{1}{2}\log(K)+O(1)\right), \tag{5.1}$$

with f *and* h *the functions defined on* $(0,1)$ *by*

$$f(x) := \log\left(x^x(1-x)^{1-x}\right)+\gamma x(1-x), \quad h(x)=\frac{1}{2}\log(x(1-x)). \tag{5.2}$$

Proof In Proposition 1, we have seen that

$$\pi_i = \frac{K!}{i!(K-i)!}\exp\left(K\gamma\frac{i}{K}\left(\frac{i}{K}-1\right)\right).$$

The term $\exp\left(K\gamma\frac{i}{K}\left(\frac{i}{K}-1\right)\right)$ corresponds to the second term $(-\gamma x(1-x))$ in the definition of $\exp\left(-f\left(\frac{i}{K}\right)\right)$. For the term $\frac{K!}{i!(K-i)!}$ we use Stirling's formula in its logarithmic form, $\log\left(n!\right)=n\log\left(n\right)-n+\frac{1}{2}\log\left(n\right)+O\left(1\right)$, to write

$$\begin{aligned}\log(K!) &= K\log(K)-K+\frac{1}{2}\log(K)+O(1),\\ -\log(i!) &= -i\log(i)+i-\frac{1}{2}\log(i)+O(1),\\ -\log((K-i)!) &= -(K-i)\log(K-i)+K-i-\frac{1}{2}\log(K-i)+O(1).\end{aligned}$$

We obtain

$$\begin{aligned}\log\frac{K!}{i!(K-i)!} &= -K\left(\left(1-\frac{i}{K}\right)\log\left(1-\frac{i}{K}\right)+\frac{i}{K}\log\left(\frac{i}{K}\right)\right)\\ &-\frac{1}{2}\log\left(\frac{i}{K}\left(1-\frac{i}{K}\right)\right)-\frac{1}{2}\log(K)+O(1),\end{aligned}$$

which ends the proof.□

Remark 2 In the approximation for $\bar{p}_i$, we need to keep $h(x)$ for the cases where i is close to 0 or close to K: in these cases we have $-h\left(x\right)=\frac{1}{2}\log\left(K\right)+O\left(1\right)$, which compensates the term $+\frac{1}{2}\log\left(K\right)$. For other values of i, it remains of order 1.

Let us study the first order continuous approximation

$$p_K(x)=\frac{e^{-Kf(x)}}{\int_0^1 e^{-Kf(y)}dy}$$

with respect to γ. The function f is symmetric with respect to $x=\frac{1}{2}$, and $f(0)=f(1)=0$. When K tends to infinity, the function $p_K(x)$ will tend to be infinite at places where $f(x)$ is minimal and 0 elsewhere, thus tending to be a sum of Dirac masses at the minimal values of f. Since f' is antisymmetric with respect to $\frac{1}{2}$ and

$$\begin{aligned}f'\left(x\right) &= -2\gamma\left(x-\frac{1}{2}\right)+\log\left(\frac{x}{1-x}\right),\quad f'\left(\frac{1}{2}\right)=0,\quad \lim_{x\to 0} f'\left(x\right)\\ &= -\infty,\quad \lim_{x\to 1} f'\left(x\right)=+\infty,\end{aligned}$$

we may have either a local minimum or maximum at $\frac{1}{2}$. The second derivative is symmetric with respect to $\frac{1}{2}$ and $f''\left(\frac{1}{2}\right)=-2\gamma+4$ is the minimal value for f''. We thus have two different cases.

- $\gamma \leq 2: x = \frac{1}{2}$ is the unique minimum of f, with $f\left(\frac{1}{2}\right) = -\log\left(2\right) + \frac{\gamma}{4}$. There is thus a unique peak of $p_K\left(x\right) \coloneqq e^{-Kf(x)}$ at $\frac{1}{2}$.
- $2 < \gamma: f$ has two local minima, at x_m and $1 - x_m$, and one local maximum at $\frac{1}{2}$. There are only two equal peaks for the function $e^{-Kf(x)}$, at the points $x_m \in \left(0, \frac{1}{2}\right)$ and $1 - x_m \in \left(\frac{1}{2}, 1\right)$.

We also notice that when γ increases, the point x_m decreases to 0, see Fig. 8b Left. The evolution of the approximate density distribution with γ is shown in Fig. 8a: we see the peaks both increasing and tending to 0 and 1. In fact it holds that $x_m \sim e^{-\gamma}$ for large γ. We also notice that an $O(e^{-\gamma})$ approximation of x_m for large γ is $1/(e^{\gamma} - 5)$ which happens to approximate x_m fairly well for all $\gamma > 2$ (Fig. 8c).

Let us now turn to a continuous approximation for the expected transition times τ_{IJ}.

Proposition 4 *Under the assumptions of Proposition* 2 *and using the definitions of* κ_k^- *and* κ_k^+ *given in* (2.3), *we obtain the following approximation of the expected transition time as* K *tends to infinity:*

$$\tau_{IJ} \approx T_{\frac{I}{K}}(J/K) \coloneqq \frac{K}{\kappa_0} \int_{I/K}^{J/K} \int_0^y \exp(-K(f(x) - f(y)))dx\,dy, \tag{5.3}$$

where $f(x)$ *is the function defined in* (5.2). *More precisely, denoting* $X = \frac{I}{K}$ *and* $Y = \frac{J-1}{K}$, *we have the following expansion*:

$$\tau_{IJ} = \frac{K}{\kappa_0} \int_X^Y \int_0^y \exp\left(-K\left(f\left(x\right) - f\left(y\right)\right) - \left(h\left(x\right) - h\left(y\right)\right) + O\left(1\right)\right) \frac{dxdy}{1-y}\left(1 + O\left(\frac{1}{K}\right)\right),$$

where $h(x)$ *is the function defined in* (5.2).

Proof We depart from the formula (3.2) of Proposition 2 defining τ_{IJ} in terms of $\overline{p}_i$, and then apply the approximate formula (5.1) for $\overline{p}_i$ (we neglect also $\exp\left(\gamma \frac{j}{k}\right)$ since it is of order 1):

$$\tau_{IJ} = \sum_{j=I}^{J-1} \sum_{i=0}^{j} \frac{\overline{p}_i}{\kappa_j^+ \overline{p}_j} = \sum_{j=I}^{J-1} \sum_{i=0}^{j} \frac{\exp\left(-Kf\left(\frac{i}{K}\right) - h\left(\frac{i}{K}\right) - \frac{1}{2}\log\left(K\right) + O\left(1\right)\right)}{\kappa_0\left(K-j\right)\exp\left(\gamma\frac{j}{K} - Kf\left(\frac{j}{K}\right) - h\left(\frac{j}{K}\right) - \frac{1}{2}\log\left(K\right) + O\left(1\right)\right)}$$

$$= \sum_{j=I}^{J-1} \sum_{i=0}^{j} \frac{1}{\kappa_0 K\left(1-\frac{j}{K}\right)} \exp\left(-K\left(f\left(\frac{i}{K}\right) - f\left(\frac{j}{K}\right)\right) - \left(h\left(\frac{i}{K}\right) - h\left(\frac{j}{K}\right)\right) + O\left(1\right)\right)$$

$$= \int_{\frac{I}{K}}^{\frac{J-1}{K}} \int_0^y \frac{K\,dx\,dy}{\kappa_0(1-y)} \exp(-K(f(x)-f(y)) - (h(x)-h(y)) + O(1))\left(1 + O\left(\frac{1}{K}\right)\right).$$

□

The approximation of the expected hitting time (3.3) through (5.3) is very accurate as illustrated in Fig. 9 for a specific choice of parameters. Note that K appears in (5.3) as a multiplying factor, which could be interpreted as a need for changing the time-scale, see e.g. Eugene et al. (2016). Less easy to interpret is the fact that K appears as a power. In our attempt to derive an approximate expression for the expected transition time we can thus go a step further, as shown by the following proposition.

6 Approximation using Laplace's method

Proposition 5 *Under the assumptions of Proposition* 4, *as both* K *and* γ *tend to infinity, the expected transition time is approximately given by:*

$$\tau_{0,J_{\max}} \approx \frac{\pi}{\kappa_0} \frac{e^{K\left(\frac{\gamma}{4} - \log(2) + e^{-\gamma}\right)}}{\sqrt{(\gamma/2-1)e^{\gamma}}}. \tag{6.1}$$

This implies that asymptotically the expected transition time grows exponentially in both K *and* γ.

Proof We use Laplace's method to approximate (5.3) for large K and large γ. Laplace's method suggests to extend the domain of integration in (5.3) to $\mathbb{R}^2$ and to simplify the integrand of (5.3) in a way which allows to compute the integral explicitly. The idea is to replace the argument of the exponential function by the parabola corresponding to the second order Taylor approximation near its peak. Since the exponential function over-weights large, positive argument, this approximates the original expression for large K although the behaviour of the integrand away from its maximum is not taken into account.

In the specific case of (5.3) the integrand can be written as $e^{f(y)-f(x)}$ with the function f defined in (5.2). A sketch of the domain of integration for arbitrary $I/K < 1/2 < J/K$ is shown in Fig. 10b. It indicates that the expression $f(y) - f(x)$ (Fig. 10a), has a well-defined

maximum at $y = x_M = 1/2$ and $x = x_m$ which correspond to the maximum and left minimum of the function f.

Writing the integrand as $e^{f(y)}/e^{f(x)}$ we also realize that the entire integral factorizes into the product of two integrals on the real line. After replacing f by its second order Taylor approximations at its maximum and minimum respectively, both integrals can be taken. This gives rise to the following computation, which reflects the Eyring-Kramers formula and which yields an approximation of (5.3) for $I/K < 1/2 < J/K$,

$$\begin{aligned}\tau_{0,J_{\max}} &\approx \frac{K}{\kappa_0}\int_{-\infty}^{\infty}\int_{-\infty}^{\infty}\left[\frac{e^{\gamma(y(1-y))}\times\left(y^y(1-y)^{1-y}\right)}{e^{\gamma(x(1-x))}\times\left(x^x(1-x)^{1-x}\right)}\right]^K dy\,dx\\ &\approx \frac{K}{\kappa_0}\int_{-\infty}^{\infty}\int_{-\infty}^{\infty}\left[\frac{\exp\left(f(x_M)+(y-x_M)^2 f''(x_M)/2\right)}{\exp\left(f(x_m)+(x-x_m)^2 f''(x_m)/2\right)}\right]^K dy\,dx\\ &= \frac{2\pi}{\kappa_0}\frac{e^{K(f(x_M)-f(x_m))}}{\sqrt{-f''(x_M)f''(x_m)}}.\end{aligned}$$

Here $x_M = 1/2$ is the (local) maximum of f and x_m denotes the local minimum of f such that $x_m \in (0,1/2)$ (see Fig. 8b).

The shape of the parabola which approximates the (local) maximum of f at 1/2 can be computed and is characterized by $f(1/2) = \gamma/4 - \log(2)$ and $f''(1/2) = 4 - 2\gamma$. The location of the minimum of f at $x_m \in (0,1/2)$ can only be computed numerically. For large γ, it is asymptotically given by $e^{-\gamma}$. This implies that $f''(x_m) \approx e^{\gamma}$ and $f(x_m) \approx e^{-\gamma}$. The resulting approximate switching time is given by Formula (6.1).□

Remark 3 As already noted, another $O(e^{-\gamma})$ approximation of x_m for large γ is $1/(e^{\gamma} - 5)$ which happens to approximate x_m fairly well for all $\gamma > 2$ (Fig. 8c). Using this approximate value and the exact formulas for f and f'', we find:

$$\tau_{0,J_{\max}} \approx \frac{\pi}{\kappa_0}\frac{e^{K\left(\frac{\gamma}{4}-\log(2)-f(x_m)\right)}}{\sqrt{(\gamma/2-1)f''(x_m)}}, \quad \text{where } x_m = \frac{1}{e^{\gamma}-5}. \tag{6.2}$$

For large enough values of γ, this is a reasonably good approximation of the switching time defined as $\tau_{0,J_{\max}}$, as shown in Fig. 11. Finally, in absolute numbers, the predicted switching times for our standard set of parameters given in Table 1 are $\tau_{0,J_{\max}} \approx 160\,\text{s}$ [resulting from (3.2)], ≈ 190 s [continuous approximation (5.3)], ≈ 157 s [close approximation (6.2)] and 103 s [rough approximation (6.1)].

7 Discussion

In this paper, we considered the tug-of-war between multiple identical molecular motors crosslinking two parallel MTs. Stochastic simulations suggest that in the limit of a great number of motors and of the detachment rate being sufficiently sensitive to the load force

($K \gg 1$, $\gamma > 2$), most of the motors at any instant are attached to just one MT with their cargo domains. Few oppositely oriented motors are attached to the same MT with their motor domains because they experience an overwhelming load force. Occasionally, a fluctuation generates a switch to the majority of the attached motors of the opposite orientation. The key to understanding the tug-of-war dynamics then is to calculate the respective switching rate. In fact, even defining what this effective switching rate between two directions means is a challenge.

We used the Master Equation describing a random walk in the space of the numbers of the opposing motors to demonstrate that the asymptotically stable motor number distribution is characterized by two sharp peaks near the ends of the motor number interval (for $\gamma > 2$ but less than a threshold value) or exactly at the ends of the interval (for γ greater than this threshold value). Furthermore, the expected time of the transition between the two directional states can be defined as the expected hitting time of the underlying Markov process of transition between two states corresponding to the peaks' maxima. We find that a valid approximation comes from calculating the expected time of the transition between the two directional states as the hitting time of a transition between a state with all motors pulling in the same direction to the equilibrium state of most (but not all) motors pulling in the other direction. Respective two states correspond to one end of the interval (all motors pulling in the same direction) and to the maximum of the opposing peak in the stationary distribution. On the other hand, the hitting time of a transition between the state with all motors pulling in the same direction to the state with all motors pulling in the opposite direction provides an inaccurate estimate for the average direction switching time.

We used explicit formula for the expected hitting times of birth and death processes and found a series of explicit formulae for the time between switching directions.We then used Laplace's method to derive the asymptotic formula for the switching frequency and found that the frequency is an exponentially decreasing function of the total motor number and of parameter γ describing the sensitivity of the motor detachment rate to the load force. This allowed us to estimate the effective diffusion coefficient for movements of the MT pair.

The question about switching frequency is linked to several characteristic timescales associated with this process. One is the relaxation time corresponding to the spectral gap of the generator, i.e. the modulus of the second largest eigenvalue of the matrix **Q**, the largest eigenvalue of which is zero. Results which elaborate on the relation include the eigenvalue identity (Aldous and Fill 2002; Miclo 2015). This question is also linked to the notion of metastability (Huisinga et al. 2004). This timescale is related to the mixing time of the process (Levin et al. 2009). Since this time is given by an eigenvalue, it is a solution of the characteristic equation which is an algebraic equation of order $K + 1$ and therefore typically does not admit a closed-form solution. Such approaches shall be studied in future work. Further study should also take into account non-instantaneous reattachment, which could explain longer pauses than our simpler model predicts.

Our analysis provides the following biological insights. First, assuming that the total motor number is proportional to the length of the MT overlap, we predict that the pair would be sliding unidirectionally for a long time if the overlap length is great, while the MTs will

switch direction of sliding often if the overlap length is short. So, effectively, the parallel MT pair is locked together, as was assumed before, but importantly, this lock is not static, but dynamic.

So far, predictions of our model were not tested directly, as it is very difficult to control the number of the crosslinking motors, as well as mechanical properties of the motor cargo domains, between the MT pairs in in vitro, and especially in in vivo experiments. However, the experiments with MT pairs being slid in vitro by collective action of multiple kinesin-14 motors were reported in (Fink et al. 2009; Ludecke et al. 2018). In these experiments, it was observed that when all motors were attached to the same MT with their cargo domain, the second MT was sliding rapidly and unidirectionally. When the motors were binding dynamically and stochastically on the other hand, low and widely distributed sliding velocities for the first 100 sec of the observation were reported. A wide distribution of low sliding velocities is similar to the diffusion behavior. The authors of these studies also hypothesized that a small number of motors were acting collectively. These observations are in qualitative agreement with the predictions of our model. Another relevant measurement, in vivo, reported a wide, mildly peaked, distribution of sliding MT velocities driven by collective dynein action in proplatelets of megakaryocyte cells (Patel et al. 2005). This result can be interpreted as follows: the velocity peak corresponds to the sliding apart of long MT pairs, while the other, widely distributed, velocities, could be generated by sliding of parallel MT pairs of variable lengths.

Although we do not explore external forces in this work, our model suggests that a shear force applied to the MT pair would not lead to an elastic response. Rather, as motors attach and reattach and the MTs slide relative to each other, our model suggests a viscous response. Such viscous-like shear is in fact consistent with observations of behavior of parallel MTs crosslinked by multiple motors (Shimamoto et al. 2015). This viscosity is likely nonlinear, as the shear would feed back mechanically to the motor directional distribution. Further modeling will be needed to estimate this effective viscosity. These conclusions will have important implications for the MT dynamics in the mitotic spindle and axon MT bundle.

Note that the original tug-of-war models assumed that both dynein and kinesin were characterized by slip-bonds (increasing detachment rate with increasing load), whereas dynein appears not to behave as a slip-bond (Kunwar et al. 2011). This calls into question the mechanism of switching for cargos driven by both dynein and kinesin. The present work applies the same notion of competing motors with slip-bonds to cases where the same species—kinesin—is in competition with itself, and where slip-bond behavior is well-established.

In the future, our analysis can be expanded to the cases when more detailed stochastic models of individual motors are used (Atzberger and Peskin 2006; Newby and Bressloff 2010; Kunwar et al. 2011; Bouzat 2016), and/or explicit thermal noise of the cargo (MTs in our case) is considered (Miles and Keener 2017). A number of recent modeling papers, in fact, addressed aspects of the tug-of-war phenomenon that are beyond the scope of our study (Zhang and Fisher 2010; Newby and Bressloff 2010; Ikuta et al. 2014; Lee and Mitchell 2015; Bhat and Gopalakrishnan 2016; Saito and Kaneko 2017). Another generalization will

be to remove the assumption that the motors reattach immediately upon detachment in a random configuration and to quantify the limitations of this simplification. Preliminary stochastic simulations where we omit this assumption show that the total number of attached motors is distributed within a narrow range around an average value. The constant K in our simplified model should therefore be identified with this average number of attached motors rather than with its maximal number.

Last, but not least, there is an important physical difference between unipolar motors, like kinesin-1 and dynein (with the cargo domain at one end and motor domain at another end), which we analyzed here, and bipolar motors, like kinesin-5 and myosin (which have effectively motor domains at both ends). For the latter, our theory will have to be modified. We emphasize though that the mathematical apparatus that we introduced here will be applicable to all these cases.

Acknowledgments

This study has been supported by NIH Grant R01 GM123068, NSF Grant DMS 1715455 and NSF Grant DMS 1763272 to JA; furthermore by ERC Starting Grant SKIPPERAD (number 306321) to MD, by ARC Discovery Project DP180102956 to DO and by NIH Grant GM121971 to AM.

References

Aldous D, Fill JA (2002) Reversible Markov chains and random walks on graphs. http://www.stat.berkeley.edu/~aldous/RWG/book.html

Anderson W (1991) Continuous-time Markov chains: an applications-oriented approach. Applied probability. Springer. ISBN 9780387973692

Atzberger PJ, Peskin CS (2006) A Brownian dynamics model of kinesin in three dimensions incorporating the force-extension profile of the coiled-coil cargo tether. Bull Math Biol 68(1):131–160 [PubMed: 16794924]

Bell G (1978) Models for the specific adhesion of cells to cells. Science 200(4342):618–627 [PubMed: 347575]

Bhat D, Gopalakrishnan M (2016) Transport of organelles by elastically coupled motor proteins. Eur Phys J E Soft Matter 39(7):71 [PubMed: 27439854]

Bouzat S (2016) Models for microtubule cargo transport coupling the Langevin equation to stochastic stepping motor dynamics: caring about fluctuations. Phys Rev E 93:012401 [PubMed: 26871095]

Craig EM, Yeung HT, Rao AN, Baas PW (2017) Polarity sorting of axonal microtubules: a computational study. Mol Biol Cell 28(23):3271–3285 [PubMed: 28978741]

del Castillo U, Winding M, Lu W, Gelfand VI (2015) Interplay between kinesin-1 and cortical dynein during axonal outgrowth and microtubule organization in Drosophila neurons. Elife 4:e10140 [PubMed: 26615019]

Eugene S, Xue W-F, Robert P, Doumic-Jauffret M (2016) Insights into the variability of nucleated amyloid polymerization by a minimalistic model of stochastic protein assembly. J Chem Phys 144(17):12

Fink G, Hajdo L, Skowronek KJ, Reuther C, Kasprzak AA, Diez S (2009) The mitotic kinesin-14 Ncd drives directional microtubule-microtubule sliding. Nat Cell Biol 11(6):717–723 [PubMed: 19430467]

Grimmett G, Grimmett P, Stirzaker D, Stirzaker M, Grimmett S (2001) Probability and random processes. OUP, Oxford. ISBN 9780198572220

Gross SP, Welte MA, Block SM, Wieschaus EF (2002) Coordination of opposite-polarity microtubule motors. J Cell Biol 156(4):715–724 [PubMed: 11854311]

Gross SP, Vershinin M, Shubeita GT (2007) Cargo transport: two motors are sometimes better than one. Curr Biol 17(12):R478–R486 [PubMed: 17580082]

Huisinga W, Meyn S, Schütte C (2004) Phase transitions and metastability in Markovian and molecular systems. ANNAP 14(1):419–458

Ikuta J, Kamisetty NK, Shintaku H, Kotera H, Kon T, Yokokawa R (2014) Tug-of-war of microtubule filaments at the boundary of a kinesin- and dynein-patterned surface. Sci Rep 4:5281 [PubMed: 24923426]

Klumpp S, Lipowsky R (2005) Cooperative cargo transport by several molecular motors. Proc Natl Acad Sci USA 102(48):17284–17289 [PubMed: 16287974]

Kunwar A, Tripathy SK, Xu J, Mattson MK, Anand P, Sigua R, Vershinin M, McKenney RJ, Yu CC, Mogilner A, Gross SP (2011) Mechanical stochastic tug-of-war models cannot explain bidirectional lipid-droplet transport. Proc Natl Acad Sci 108(47):18960–18965 [PubMed: 22084076]

Kural C, Kim H, Syed S, Goshima G, Gelfand VI, Selvin PR (2005) Kinesin and dynein move a peroxisome in vivo: a tug-of-war or coordinated movement? Science 308(5727):1469–1472 [PubMed: 15817813]

Lee RH, Mitchell CS (2015) Axonal transport cargo motor count versus average transport velocity: is fast versus slow transport really single versus multiple motor transport? J Theor Biol 370:39–44 [PubMed: 25615423]

Levin DA, Peres Y, Wilmer EL (2009) Markov chains and mixing times. American Mathematical Society, Providence

Lu W, Gelfand VI (2017) Moonlighting motors: kinesin, dynein, and cell polarity. Trends Cell Biol 27(7):505–514 [PubMed: 28284467]

Lu W, Fox P, Lakonishok M, Davidson MW, Gelfand VI (2013) Initial neurite outgrowth in Drosophila neurons is driven by kinesin-powered microtubule sliding. Curr Biol 23(11):1018–1023 [PubMed: 23707427]

Ludecke A, Seidel AM, Braun M, Lansky Z, Diez S (2018) Diffusive tail anchorage determines velocity and force produced by kinesin-14 between crosslinked microtubules. Nat Commun 9(1):2214 [PubMed: 29880831]

McKinley SA, Athreya A, Fricks J, Kramer PR (2012) Asymptotic analysis of microtubule-based transport by multiple identical molecular motors. J Theor Biol 305:54–69 [PubMed: 22575549]

Miclo L (2015) An absorbing eigentime identity. Markov Proc Relat Fields 21(2):249–262

Miles CE, Keener JP (2017) Bidirectionality from cargo thermal fluctuations in motor-mediated transport. J Theor Biol 424:37–48 [PubMed: 28472620]

Müller MJI, Klumpp S, Lipowsky R (2008) Tug-of-war as a cooperative mechanism for bidirectional cargo transport by molecular motors. Proc Natl Acad Sci 105(12):4609–4614 [PubMed: 18347340]

Nascimento AA, Roland JT, Gelfand VI (2003) Pigment cells: a model for the study of organelle transport. Annu Rev Cell Dev Biol 19:469–491 [PubMed: 14570578]

Newby JM, Bressloff PC (2010) Quasi-steady state reduction of molecular motor-based models of directed intermittent search. Bull Math Biol 72(7): 1840–1866 [PubMed: 20169417]

Norris JR (1997) Markov chains. Cambridge series in statistical and probabilistic mathematics. Cambridge University Press, Cambridge

Oelz DB, Del Castillo U, Gelfand VI, Mogilner A (2018) Microtubule dynamics, kinesin-1 sliding, and dynein action drive growth of cell processes. Biophys J 115(8):1614–1624 [PubMed: 30268540]

Patel SR, Richardson JL, Schulze H, Kahle E, Galjart N, Drabek K, Shivdasani RA, Hartwig JH, Italiano JE (2005) Differential roles of microtubule assembly and sliding in proplatelet formation by megakaryocytes. Blood 106(13):4076–4085 [PubMed: 16118321]

Rogers SL, Gelfand VI (2000) Membrane trafficking, organelle transport, and the cytoskeleton. Curr Opin Cell Biol 12(1):57–62 [PubMed: 10679352]

Saito N, Kaneko K (2017) Embedding dual function into molecular motors through collective motion. Sci Rep 7:44288 [PubMed: 28281683]

Saloff-Coste L (1997) Lectures on finite Markov chains. In: Bernard P (ed) Lectures on probability theory and statistics. Lecture notes in mathematics, vol 1665. Springer, Berlin, pp 301–413

Sharp DJ, Brown HM, Kwon M, Rogers GC, Holland G, Scholey JM (2000) Functional coordination of three mitotic motors in Drosophila embryos. Mol Biol Cell 11(1):241–253 [PubMed: 10637305]

Shimamoto Y, Forth S, Kapoor TM (2015) Measuring pushing and braking forces generated by ensembles of kinesin-5 crosslinking two microtubules. Dev Cell 34(6):669–681 [PubMed: 26418296]

Svoboda K, Block SM (1994) Force and velocity measured for single kinesin molecules. Cell 77(5):773–784 [PubMed: 8205624]

Visscher K, Schnitzer MJ, Block SM (1999) Single kinesin molecules studied with a molecular force clamp. Nature 400(6740): 184–189 [PubMed: 10408448]

Wollman R, Civelekoglu-Scholey G, Scholey JM, Mogilner A (2008) Reverse engineering of force integration during mitosis in the Drosophila embryo. Mol Syst Biol 4:195 [PubMed: 18463619]

Zhang Y, Fisher ME (2010) Dynamics of the tug-of-war model for cellular transport. Phys Rev E Stat Nonlinear Soft Matter Phys 82(1 Pt 1):011923

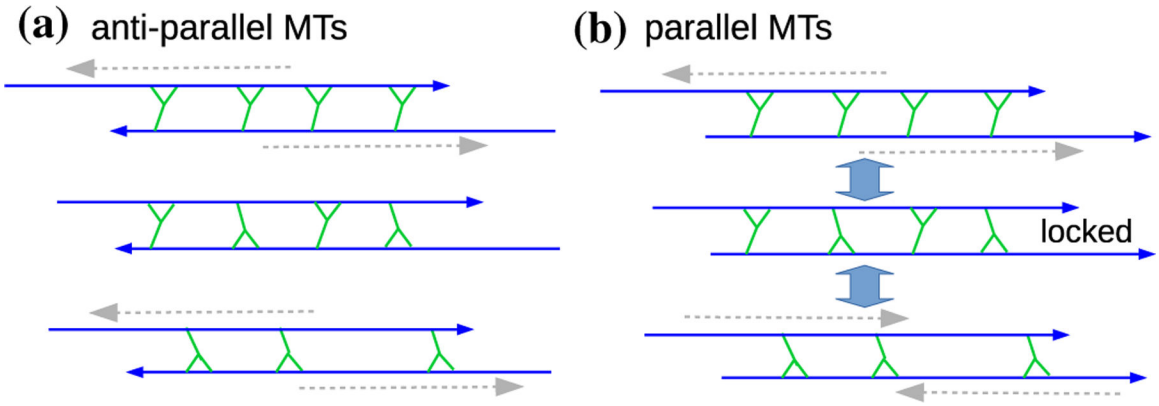

Fig. 1.

Tug-of-war. Molecular motor proteins are represented by green forks. The symbol is indeed the letter Y if the motor domain is attached to the upper fiber (in blue) with the cargo domain attached to the lower fiber. The symbol is an upside-down Y in case the motor domain is attached to the lower fiber with the cargo domain attached to the upper one. The motor domains move to the plus end of the respective fiber symbolized by an arrowhead. This slides the fibers in a way which depends on their relative polarity. **a** MTs are anti-parallel: fibers move in the direction of their minus end irrespective of the direction of motor proteins. **b** MTs are parallel (here with the plus ends to the right): the fiber to which the higher number of motor domains is attached moves to the left (dotted gray arrows), while the other one slides to the right. Only with an equal number of motors in both directions the pair of fibers is locked and therefore does not move

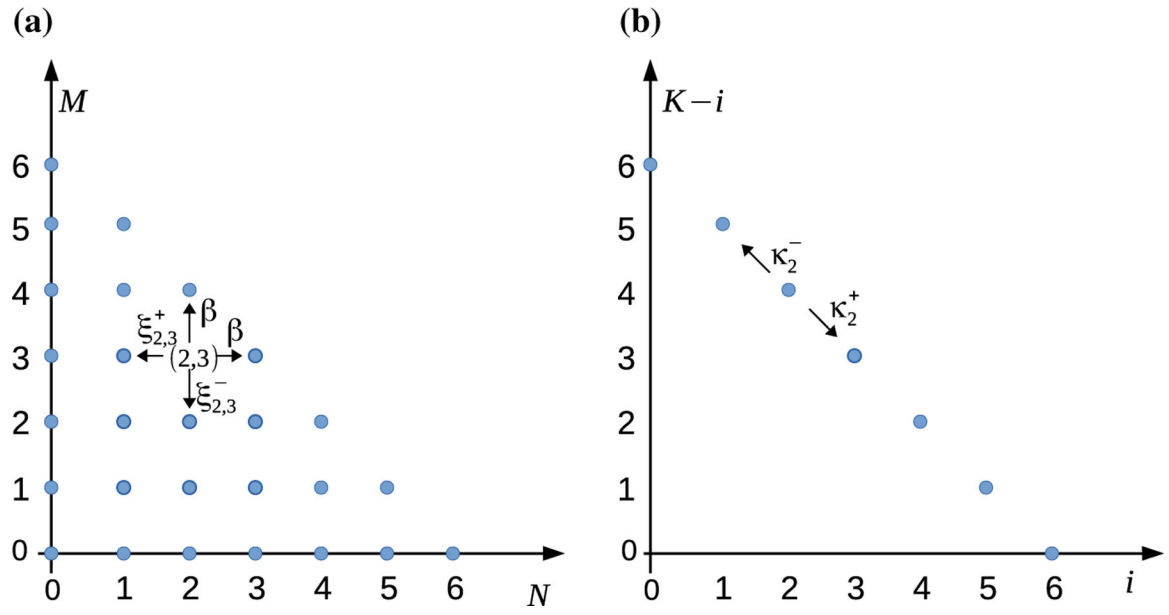

Fig. 2.

a Sketch of the general mathematical model, here shown for $K = 6$. **b** In the limit when reattachment is fast, the state space is restricted to $N + M = K$. In this case the mathematical model is a classical birth–death process with transition rates $\kappa_i^{\pm}$

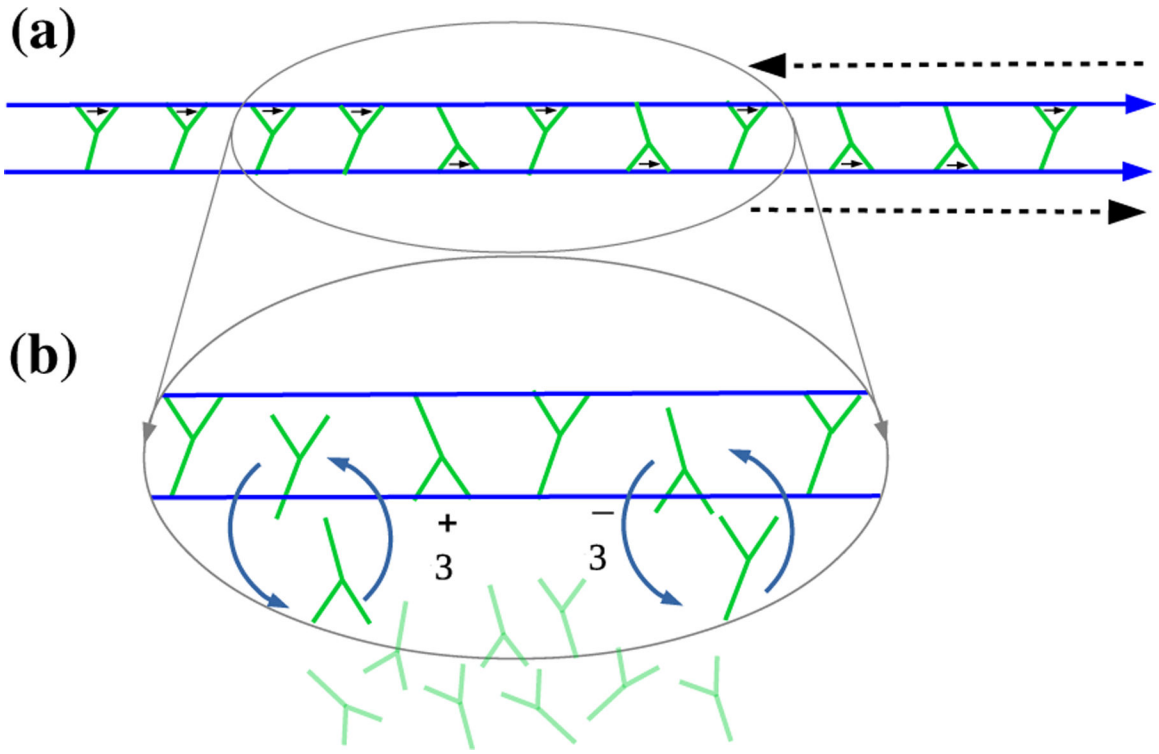

Fig. 3.
Sketch of the mathematical model **a** $K = 11$, $i = 4$, which implies $K - i = 7$. **b** Detailed visualization of turnover

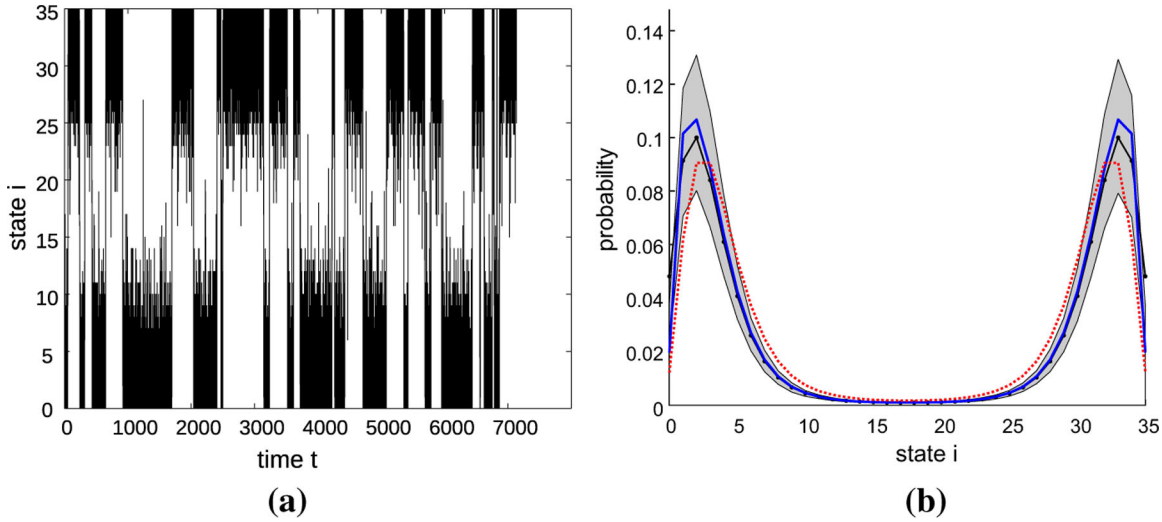

Fig. 4.

Stochastic simulations by a Gillespie's algorithm for $K = 35$, $\gamma = 3$ and $\kappa_0 = 1/2$. **a** One out of the 100 Gillespie simulations. Average number of transitions (from state 0 to state K or the reverse) for each simulation run: 45.3 ± 7.5. Average time-span of simulation runs: 7145 ± 32.6. Average duration of transitions between states 0 and K: 162 ± 29.9. **b** Visualization of the stationary distribution $\overline{\mathbf{p}}$ (black line and dots), compared with the first order approximate formula $p_K = e^{-Kf}$ (dotted red line) and the second order approximate formula $e^{-Kf-h-\frac{1}{2}\log\left(K\right)}$ (full blue). The grey area shows the zone where 95% out of 100 repeated stochastic simulations of 3.10^6 reaction steps lie

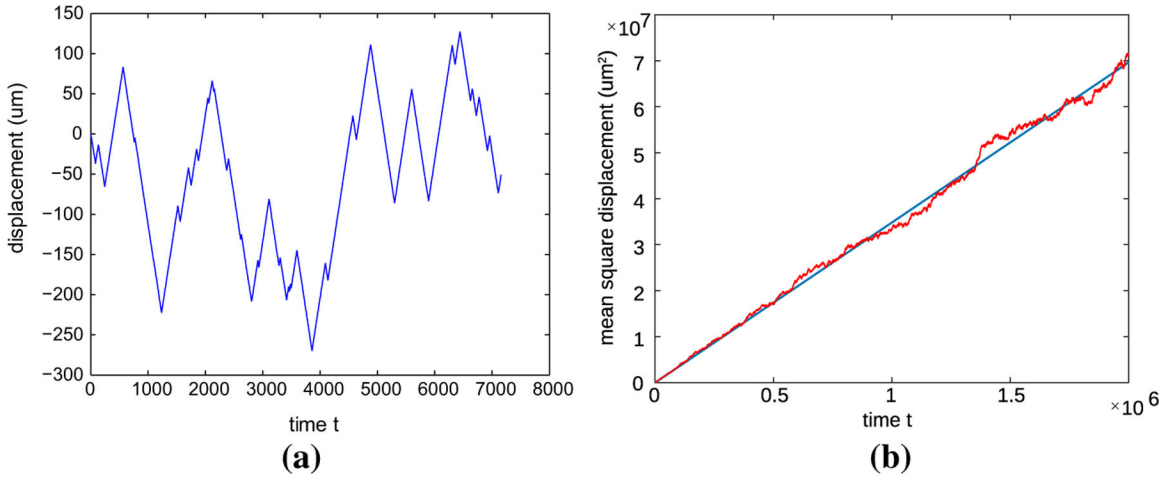

Fig. 5.

Stochastic simulations for $K = 35$, $\gamma = 3$ and $\kappa_0 = 1/2$: **a** relative displacement of the two MYs simulated as shown in Fig. 4a. The relative displacement is updated in every timestep by $\Delta t \times \Delta v$ with the relative velocity given by (2.1). **b** Mean squared displacement $\langle x(t)^2 \rangle$ vs time (red) for 200 simulation runs with the same parameter set. The linear regression line is shown in blue

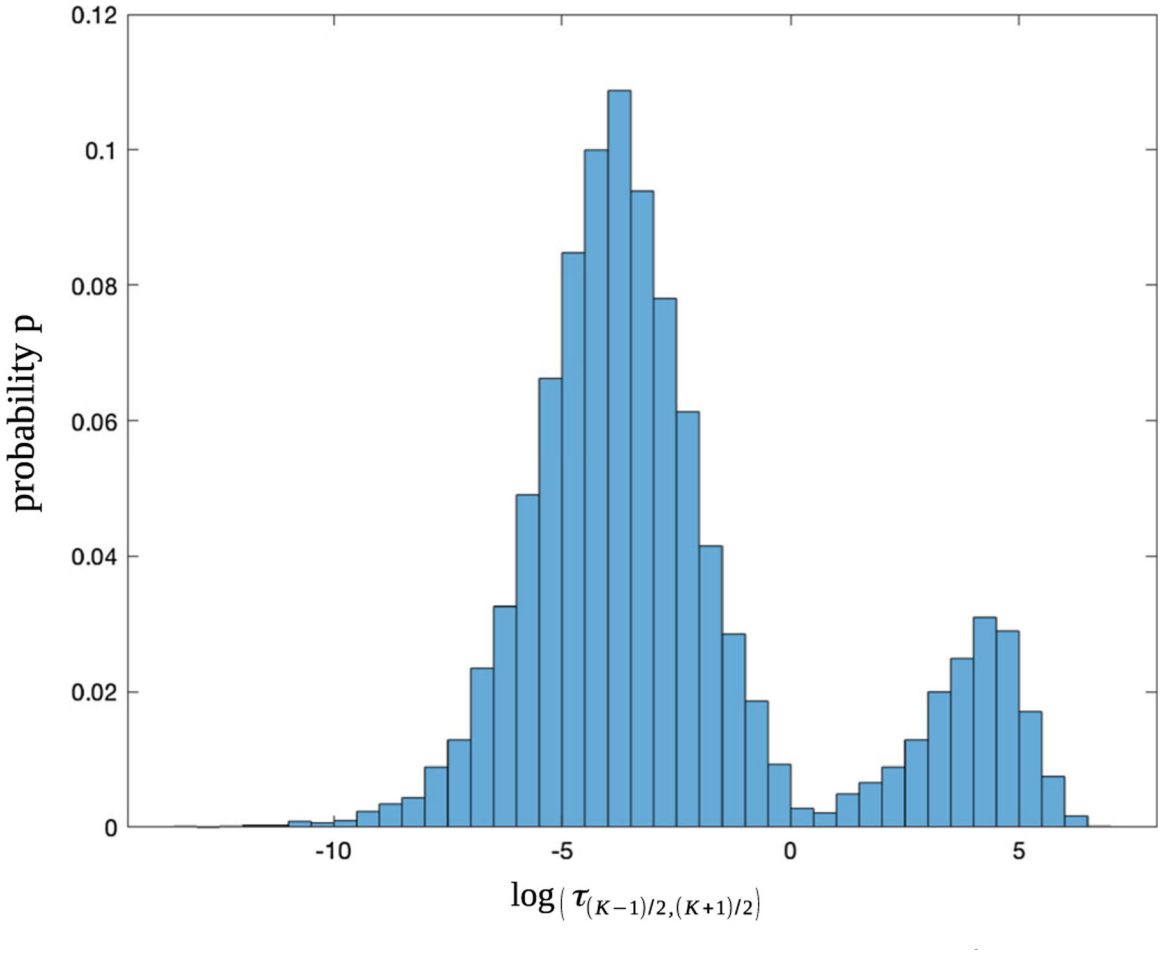

Fig. 6.

Stochastic simulation for parameter values $K = 35$, $\gamma = 3$ and 3×10^6. Histogram of simulated hitting times (logarithmic scale) to go from state $(K - 1)/2$ to state $(K + 1)/2$. The bimodal distribution corresponds to one group of very fast transitions and another group of slow transitions (the latter are of characteristic duration of e^5 corresponding to approximately 148 sec real time

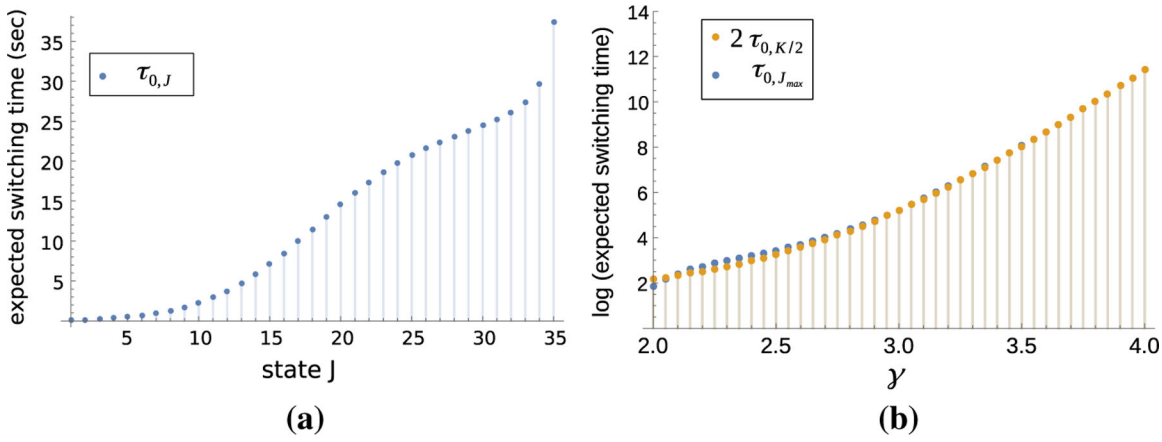

Fig. 7.

a τ_{0J} as a function of the state $0 \leq J \leq K$ for $\gamma = 2.5$. **b** Log of approximated switching times for $K = 35$ as function of γ. We compare the approximated switching time $\tau_{0,J_{\max}}$ where the state $J_{\max}$ is the maximum of the stationary distribution (blue) and $2\tau_{0,K/2}$ where $\tau_{0,K/2}$ is the expected time to go from the left extreme state to the central transition state (orange)

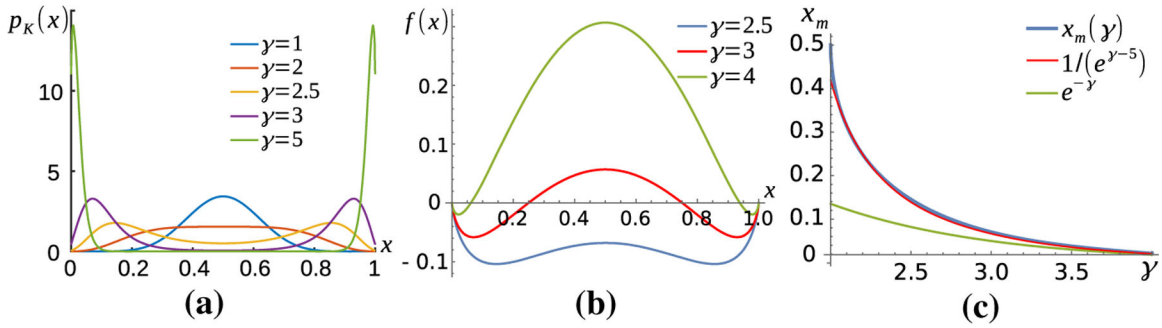

Fig. 8.

$K = 35$, and $\kappa_0 = 1/2$: **a** the limit density $p_K(x)$, here with $K = 35$, for various values of γ. **b** Graph of f for $\gamma = 2.5$ (blue), $\gamma = 3$ (red) and $\gamma = 4$ (green). **c** Location of the left local minimum. blue: exact value $x_m(\gamma) \in (0,1/2)$, red: $1/(e^{\gamma} - 5)$, green: $e^{-\gamma}$

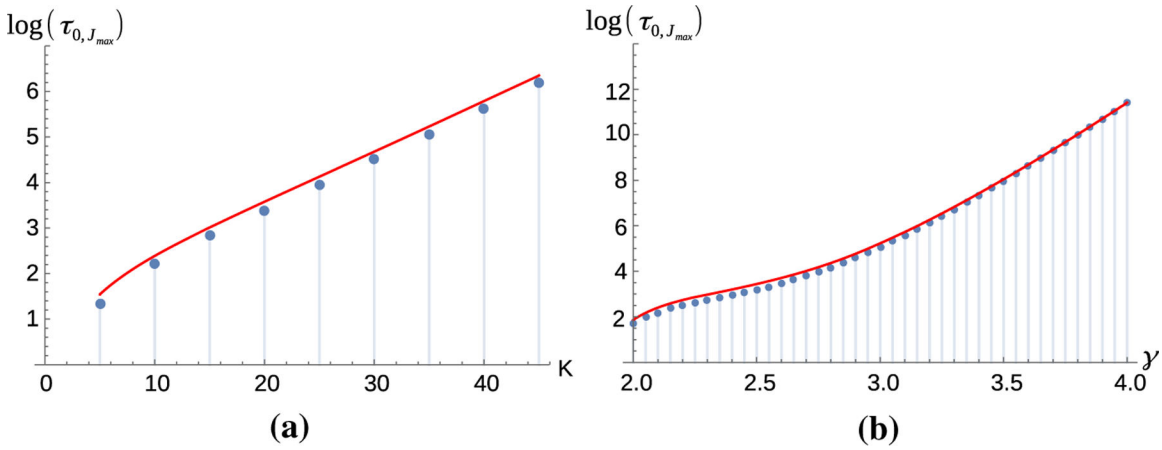

Fig. 9.

Log-plots of $\tau_{0,J\max}$ (blue dots) and its approximation (5.3) (red graph). **a** Comparison for $\gamma = 3$ as a function of K. **b** Comparison for $K = 35$ as a function of γ

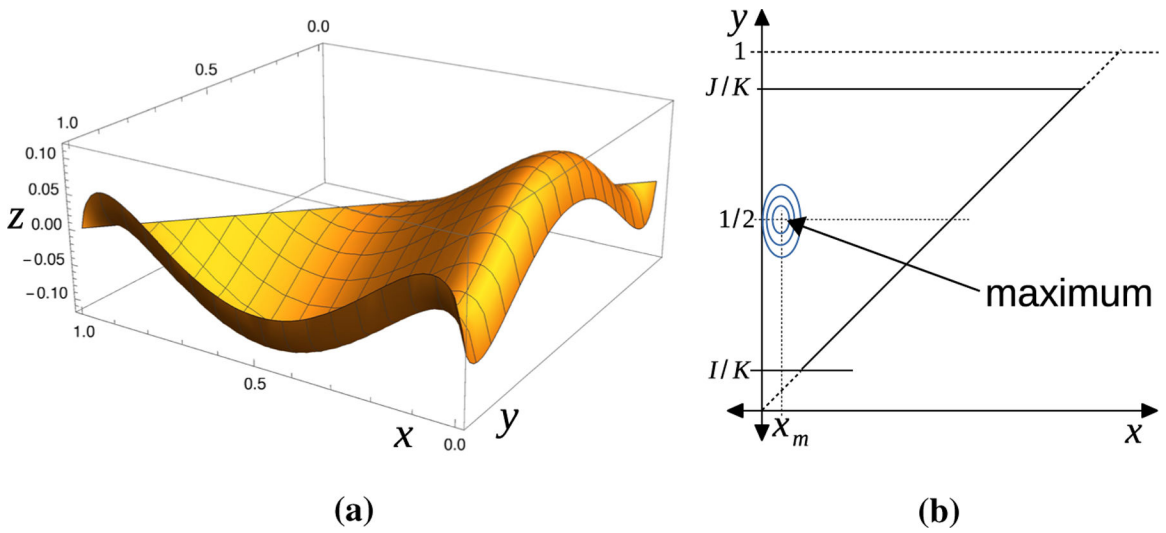

Fig. 10.

a Plot of $f(y) - f(x)$ where $e^{f(y) - f(x)}$ is the integrand in (5.3) for $K = 35, \kappa_0 = 1/2$ and $\gamma = 3$ on the maximal domain of integration where $I/K = 0$ and $J/K = 1$. **b** Domain of integration in (5.3). Note that the peak shown in **a** is located at $y = 1/2, x = x_m$ and included in the domain of integration of any $I/K < 1/2 < J/K$

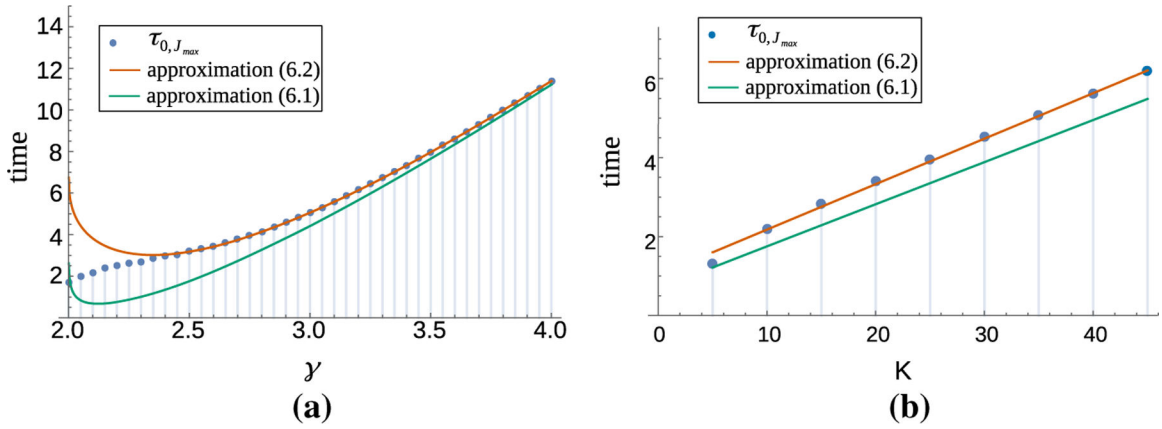

Fig. 11.

Log-plots of approximate hitting time $\tau_{0,}J_{\max}$ (blue dots) and the approximation due to the Laplace method with the exact minimum of f (6.2) (red) and with the approximate minimum of f (6.1) (green). **a** Comparison for $K = 35$ and $\kappa_0 = 1/2$ as a function of γ. **b** Comparison for $\gamma = 3$ and $\kappa_0 = 1/2$ as a function of K

Table 1

List of parameters and their orders of magnitude

Description	Symbol	Value	References
Stall force (kinesin)	F_s	6 pN	Visscher et al. (1999)
Detachment force (kinesin)	f_0	4 pN	Kunwar et al. (2011)
Free moving velocity (kinesin)	V_m	0.57 μms^{-1}	Kunwar et al. (2011)
Number of competing motor proteins	K	35	Value used for testing
Force-less detachment rate	$\overline{\kappa}_0$	1 s^{-1}	Kunwar et al. (2011)
Force-less transition rate	κ_0	0.5s^{-1}	Equal probability of another motor to attach in either direction
Scaled, dimensionless stall force	γ	3	$\gamma = 2F_s/f_0$

Table 2

Comparison of the diffusion coefficients observed in stochastic simulations (slope according to linear regression line as illustrated in Fig. 5b) and estimated as $\frac{1}{2} \times$ mean rel. velocity × run length where run length $= \tau_K - J_{\max}, J_{\max} \times$ mean rel. velocity for several values of the scaled load-sensitivity γ

γ	D (μm^2/s)	$D_{estimate}$ (μm^2/s)
0	7.6×10^{-3}	$1.6 \times 10^{-3} - 24 \times 10^{-3}$
2	0.14	0.09
2.5	1.33	2.4
3	17.4	20.6
4	12.1×10^{3}	14.4×10^{3}